FULL PAPER

Dalton
www.rsc.org/dalton

Synthesis, characterisation and catalytic potential of hydrazonato-vanadium(V) model complexes with $[VO]^{3+}$ and $[VO_2]^{+}$ cores†

Mannar R. Maurya,*[a] Shalu Agarwal,[a] Cerstin Bader,[b] Martin Ebel[b] and Dieter Rehder[b]

[a] *Department of Chemistry, Indian Institute of Technology Roorkee, Roorkee, 247 667, India. E-mail: rkmanfcy@iitr.ernet.in*

[b] *Institut für Anorganische und Angewandte Chemie, Universität Hamburg, Martin-Luther-King-Platz 6, 20146, Hamburg, Germany. E-mail: dieter.rehder@chemie.uni-hamburg.de*

Received 21st October 2004, Accepted 14th December 2004
First published as an Advance Article on the web 10th January 2005

Reaction between $[VO(acac)_2]$ and H_2L (H_2L are the hydrazones H_2sal-nah **I** or H_2sal-fah **II**; sal = salicylaldehyde, nah = nicotinic acid hydrazide and fah = 2-furoic acid hydrazide) in methanol leads to the formation of oxovanadium(IV) complexes $[VOL{\cdot}H_2O]$ (H_2L = **I**: **1**, H_2L = **II**: **4**). Aerial oxidation of the methanolic solutions of **1** and **4** yields the dinuclear oxo-bridged monooxovanadium(V) complexes $[\{VOL\}_2\mu\text{-}O]$ (H_2L = **I**: **2**, H_2L = **II**: **5**). These dinuclear complexes slowly convert, in excess methanol, to [VO(OMe)(MeOH)L] (H_2L = **I**: **9**, H_2L = **II**: **10**), the crystal and molecular structures of which have been determined, confirming the ONO binding mode of the dianionic ligands in their enolate form. Reaction of aqueous $K[VO_3]$ with the ligands at pH *ca.* 7.5 results in the formation of $[K(H_2O)][VO_2L]$ (H_2L = **I**: **3**, H_2L = **II**: **6**). Treatment of **3** and **6** with H_2O_2 yields (unstable) oxoperoxovanadium(V) complexes $K[VO(O_2)L]$, the formation of which has been monitored spectrophotometrically. Acidification of methanolic solutions of **3** and **6** with HCl affords oxohydroxo complexes, while the neutral complexes $[VO_2$(Hsal-nah)] **7** and $[VO_2$(Hsal-fah)] **8** were isolated on treatment of aqueous solutions of **3** and **6** with $HClO_4$. These complexes slowly transform into **9** and **10** in methanol, as confirmed by ^{1}H, ^{13}C and ^{51}V NMR. The anionic complexes **3** and **6** catalyse the oxidative bromination of salicylaldehyde in water in the presence of H_2O_2/KBr to 5-bromosalicylaldehyde and 3,5-dibromosalicylaldehyde, a reaction similar to that exhibited by vanadate-dependent haloperoxidases. They are also catalytically active for the oxidation of benzene to phenol and phenol to catechol and *p*-hydroquinone.

Introduction

The stabilization, under aerobic conditions, of vanadium(V) complexes with a mixed ON coordination sphere[1–3] is of topical interest because of the potential of these complexes as structural and/or functional models for vanadate-dependent haloperoxidases (VHPO).[4–9] In VHPO, vanadium is in a trigonal-bipyramidal (native form) or tetragonal-pyramidal (peroxo form) environment, covalently linked to the Nε of a histidine.[4,10,11] These enzymes catalyse the oxidation, by peroxide, of halides to hypohalous acid which further halogenates hydrocarbons non-enzymatically. Vanadium(V) complexes have also been shown to act as electron acceptors and thus initiators in the photo-cleavage of DNA.[12] Further, many vanadium complexes show catalytic activity in oxidation and oxygen transfer reactions,[13,14] including the oxidation of (prochiral) organic sulfides to (chiral) sulfoxides.[15–18] Oxidation reactions of various organic substrates by peroxides, catalysed by vanadium complexes, have been reviewed.[19]

We recently reported on structural models of VHPO, *viz.* dioxovanadium(V) complexes of ONO donor ligands based on salicylidenehydrazides, and demonstrated their ability to transfer, *via* an oxo-peroxo intermediate, an oxo group to a substrate such as PPh_3.[20] Anionic and neutral *cis*-dioxovanadium(V) complexes containing the tridentate *N*-salicylidenehydrazide ligand system, and their model character for VHPO have recently been reviewed by Plass.[21] The objective of the present work is to synthesise mononuclear dioxovanadium(V) and dinuclear μ-oxo-bis{oxovanadium(V)} complexes of the hydrazones **I** and **II** formed from salicylaldehyde (Hsal) and nicotinic acid hydrazide (Hnah) or 2-furoic acid hydrazide (Hfah), Scheme 1. Their conversion to complexes containing the {VO(OH)} and $\{VO(O_2)\}$ cores, and thus mimicking active site features of VHPO, will be addressed. The isolation of complexes with the {VO(OMe)} core from $\{VO_2\}$ and $\{\mu\text{-}O(VO)_2\}$ type complexes is of particular interest in the context of oxo transfer catalysis. The knowledge on alkoxo-oxovanadium(V) complexes so far is sparse.[20,22–29]

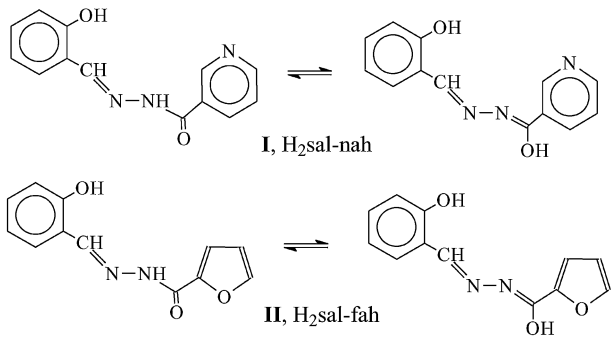

Scheme 1

Experimental

Materials and methods

V_2O_5, nicotinic acid hydrazide, 2-furoic acid hydrazide (Fluka Chemie, Switzerland), acetylacetone (Hacac) (Aldrich, USA), salicylaldehyde (Hsal), phenol, benzene, 30% aqueous H_2O_2 and 70% $HClO_4$ (Qualigens, India) were used as obtained. Other chemicals and solvents were of analytical reagent grade. H_2sal-fah[30] and $[VO(acac)_2]$[31] were prepared according to methods

† Electronic supplementary information (ESI) available: Fig. S1: Magnetic susceptibility *vs.* temperature for **1**; detailed description of IR spectra; Table S1: ^{1}H NMR chemical shifts; Table S2: ^{13}C NMR chemical shifts; Table S3: Electronic absorption spectra. See http://www.rsc.org/suppdata/dt/b4/b416292g/

DOI: 10.1039/b416292g

reported in the literature. H_2sal-nah was prepared following the procedure reported for H_2sal-fah.

Elemental analyses of the ligands and complexes were performed by the micro-analytical section of the Central Drug Research Institute, Lucknow, India. IR spectra were recorded as KBr pellets on a Perkin-Elmer model 1600 FT-IR spectrometer. Electronic absorption spectra were measured in methanol or DMF with an UV-1601 PC UV-Vis spectrophotometer. ^{1}H NMR spectra were obtained on a Bruker 200, and ^{51}V NMR spectra on a Bruker Avance 400 MHz spectrometer at 94.73 MHz with the common parameter settings. NMR spectra were usually recorded in DMSO-d_6, and $\delta(^{51}V)$ values are referenced relative to $VOCl_3$ as external standard. Selected ^{1}H NMR and ^{51}V NMR results have also been obtained in CD_3OD. Thermogravimetric analyses of the complexes were carried out under oxygen atmosphere using a TG Stanton Redcroft STA 780 instrument. The magnetic susceptibilities were measured by a Vibrating Sample Magnetometer model 155, using nickel as standard. Susceptibilities were measured in the temperature range 298–78 K while applying a magnetic field of 0.5 T. Diamagnetic corrections were carried out using Pascal's increments.[32] EPR spectra were recorded with a Bruker ESP 300E spectrometer between 9.42 and 9.47 GHz, and EPR parameters were adjusted by simulation with the Bruker program system SimFonia.

The reaction product obtained from the catalytically conducted oxidative bromination of salicylaldehyde and oxidation of benzene as well as phenol were analysed using a Hewlett Packard 5890 A gas chromatograph fitted with FID detector and a stainless steel column HP 1. The identities of the brominated products were confirmed by the GC-MS reference system Shimadzu QP-5000.

Crystal structure determinations

Data were collected on a Bruker SMART CCD Apex diffractometer at 153(2) K, using graphite-monochromated Mo-Kα radiation (λ = 0.71073 Å). H atoms (except of the methanol-OH) were placed into calculated positions and included in the last cycles of refinement. The proton on O5 was found. Crystal data and details on the data collection and refinement are collated in Table 1. The program system SHELXTL 5.1 was used throughout. Disorder of the furfuryl ring atoms C3 and O6 of compound **10** over two alternative positions was treated with a 1 : 1 model.

CCDC reference numbers 252201 (**9**) and 251548 (**10**).

See http://www.rsc.org/suppdata/dt/b4/b416292g/ for crystallographic data in CIF or other electronic format.

Preparations

[VO^{IV}(sal-nah)H$_2$O] 1 and [{V^{V}O(sal-nah)}$_2$μ-O] 2. A filtered solution of H_2sal-nah (0.480 g, 0.002 mol) in methanol (20 ml) was added with stirring to a solution of [VO(acac)$_2$] (0.530 g, 0.002 mol) dissolved in methanol (20 ml), and the resulting reaction mixture was refluxed on a water bath for 6 h. After cooling to room temperature, a greenish-yellow precipitate of **1** was filtered off, washed with methanol and dried. Compound **1** was suspended in methanol (40 ml) and air was passed through the suspension for up to 20 h with occasional shaking, until precipitation of crystalline brown solid **2** occurred. This was filtered off, washed with methanol and dried *in vacuo*. For the preparation of **2**, it is not necessary to isolate **1**. Data for **1**: Yield 0.38 g (62.3%) (Found: C, 48.38; H, 3.26; N, 13.13. Calc. for $C_{13}H_{11}N_3O_4V$ (324.19 g mol^{-1}): C, 48.15; H, 3.42; N, 12.97%). IR (KBr, ν_{max}/cm^{-1}): 1608 (C=N$_{azomethine}$), 1285 (C–O$_{enolate}$), 1046 (N–N), 988 (V=O). μ_{eff} (293 K) = 1.54 μ_B. Data for **2**: Yield (based on [VO(acac)$_2$]): 0.48 g (38.2%) (Found: C, 48.35; H, 3.0; N, 12.12. Calc. for $C_{26}H_{18}N_6O_7V_2$ (628.01 g mol^{-1}): C, 49.70; H, 2.89; N 13.37%). IR (KBr, ν_{max}/cm^{-1}): 1607 (C=N$_{azomethine}$), 1279 (C–O$_{enolate}$), 1048(N–N), 968 (V=O), 850 [V–(μ-O)–V]. ^{51}V NMR (DMSO-d_6, δ/ppm): −542.4 and minor signal at −584; (CD_3OD): −541.7 and a minor signal at −550.1.

[K(H$_2$O)][V^{V}O$_2$(sal-nah)] 3. Vanadium(V) oxide (0.91 g, 0.005 mol) was suspended in aqueous KOH (0.28 g, 0.005 mol in 10 ml H_2O) and stirred for 2 h at 50 °C. The resulting solution was filtered. A filtered solution of H_2sal-nah (1.20 g, 0.005 mol), dissolved in 20 ml of aqueous KOH (0.56 g, 0.010 mol), was added with stirring, and the pH of the reaction mixture was slowly adjusted to 7.5 with 4 M HCl. After 2 h of stirring, a yellow solid had formed, which was filtered off, washed with cold water and dried. The solid material was redissolved in *ca.* 25 ml of methanol and kept at 10 °C. Within 2–4 days, **3** precipitated as a yellow solid, which was filtered off and dried *in vacuo* over silica gel. Yield: 0.31 g (41%) (Found: C, 42.0; H, 2.76; N, 10.95. Calc. for $C_{13}H_{11}KN_3O_5V$ (378.98 g mol^{-1}): C, 41.17; H, 2.93; N 11.08%). IR (KBr, ν_{max}/cm^{-1}): 1619 (C=N$_{azomethine}$), 1224 (C–O$_{enolate}$), 1028 (N–N), 917, 935 (sym and antisym VO_2^+). ^{51}V NMR (DMSO-d_6, δ/ppm): −532.4.

[V^{IV}O(sal-fah)H$_2$O] 4 and [{V^{V}O(sal-fah)}$_2$μ-O] 5. Complexes **4** and **5** were prepared analogously to **1** and **2**, replacing H_2sal-nah for H_2sal-fah. Data for **4**: Yield: 0.40 g (68.0%) (Found: C, 46.29; H, 3.02; N, 9.18. calc. for $C_{12}H_{10}N_2O_5V$ (313.00 g mol^{-1}): C, 46.01; H, 3.22, N, 8.95%). IR (KBr, ν_{max}/cm^{-1}): 1613 (C=N$_{azomethine}$), 1222 (C–O$_{enolate}$), 1030 (N–N), 966 (V=O). μ_{eff} (293 K) = 1.48 μ_B. Data for **5**: Yield 0.50 g (41.0%) (Found: C, 46.06; H, 3.76; N, 7.54. Calc. for $C_{24}H_{16}N_4O_9V_2$ (605.98 g mol^{-1}): C, 47.53; H, 2.66; N, 9.24%). IR (KBr, ν_{max}/cm^{-1}): 1611 (C=N$_{azomethine}$), 1281 (C–O$_{enolate}$), 1029 (N–N), 964 (V=O), 757 [V–(μ-O)–V]. ^{51}V NMR (DMSO-d_6, δ/ppm): −536.6, −548.4 and −585.6.

Table 1 Crystal data and structure refinement for [VO(OMe)(MeOH)(sal-nah)] (**9**) and [VO(OMe)(MeOH)(sal-fah)] (**10**)

	9	**10**
Empirical formula	$C_{30}H_{32}N_6O_{10}V_2$	$C_{28}H_{28}N_4O_{12}V_2$
M	738.50	714.42
Crystal system, space group	Monoclinic, *P*2(1)/*c*	Monoclinic, *P*2(1)/*c*
a/Å	8.0161(2)	8.3650(3)
b/Å, *β*/°	14.9534(4), 92.9190(10)	16.0241(5), 104.4460(10)
c/Å	13.2937(4)	11.7780(4)
V/Å^3	1591.42(8)	1528.83(9)
Z	2	2
ρ_{calc}/g cm^{-3}	1.541	1.556
μ/mm^{-1}	0.654	0.681
F(000)	760	736
Reflections collected/unique	41950/5507	15273/2659
R(int)	0.0436	0.0338
Data/restraints/parameters	5507/0/281	2659/0/210
Goodness-of-fit on F^2	1.151	1.214
R indices, [$I > 2\sigma(I_0)$]: *R*1, *wR*2	0.0378, 0.0962	0.0467, 0.1505
R indices (all data): *R*1, *wR*2	0.0395, 0.0976	0.0491, 0.1535

[K(H$_2$O)][V^{V}O$_2$(sal-fah)] 6. This complex was prepared from KVO_3 and H_2sal-fah by the method outlined for **3**. The crude material was dissolved by heating in a minimum amount of methanol and filtered. On keeping 2–4 days at *ca.* 10 °C, **6** precipitated as a brown solid. This was filtered off and dried *in vacuo* over silica gel. Yield 0.29 g (39.4%) (Found: C, 38.91; H, 2.86; N, 7.38. Calc. for $C_{12}H_{10}KN_2O_6V$ (367.96 g mol^{-1}): C, 39.13; H, 2.74; N 7.61%). IR (KBr, ν_{max}/cm^{-1}): 1620 (C=N$_{azomethine}$), 1224 (C–O$_{enolate}$), 1037 (N–N), 905, 935 (sym and antisym VO_2^+). ^{51}V NMR (DMSO-d$_6$, δ/ppm): −533.9.

[V^{V}O$_2$(Hsal-nah)] 7 and [V^{V}O$_2$(Hsal-fah)] 8. 1 mmol of complex **3** or **6** was dissolved in water (40 ml) and treated dropwise with aqueous $HClO_4$ (2 ml of 70% $HClO_4$ diluted with 5 ml of water) with stirring until most of the complex had precipitated as a yellow solid. After 1 h of stirring, the solution was filtered, the residue washed with water and dried *in vacuo* over silica gel. Similar results were also obtained with HCl. Data for **7**: Yield: 0.14 g (43.3%). IR (KBr, ν_{max}/cm^{-1}): 3090 (NH), 1606 (C=N$_{azomethine}$), 1220 (C–O$_{enolate}$), 1024 (N–N), 909, 940 (sym and antisym VO_2^+). Data for **8**: Yield: 0.15 g (48.1%). IR (KBr, ν_{max}/cm^{-1}): 3108 (NH), 1618 (C=N$_{azomethine}$), 1221 (C–O$_{enolate}$), 1016 (N–N), 942, 966 (sym and antisym VO_2^+). ^{51}V NMR of the crude sample (DMSO-d$_6$, δ/ppm): −551.0, −584.0. ^{51}V NMR of **8** recrystallised from methanol (DMSO-d$_6$, δ/ppm): −538.7, −550.5 and −583.5.

[V^{V}O(OMe)(MeOH)(sal-nah)] 9 and [V^{V}O(OMe)(MeOH)-(sal-fah)] 10. Crystals of **9** and **10** suitable for an X-ray analysis were grown from a dilute solution of **1** and **4** or **7** and **8** in methanol. The solutions were allowed to stand for slow evaporation at *ca.* 10 °C, whereupon dark brown crystals of **9** or **10** slowly separated out within 2–4 weeks.

Catalytic reactions

Oxidative bromination of salicylaldehyde. Complexes **3** and **6** were used as catalysts to carry out oxidative bromination. In a typical reaction, salicylaldehyde (0.244 g, 2 mmol) was added to an aqueous solution (4 ml) of KBr (0.476 g, 4 mmol), followed by addition of aqueous 30% H_2O_2 (1.42 g, 15 mmol) in a 50 ml reaction flask. The catalyst (0.02 g) and 70% $HClO_4$ (1 mmol) were added, and the reaction mixture was stirred at room temperature. Three additional 1 mmol portions of 70% $HClO_4$ were further added to the reaction mixture in three equal portions in half hour intervals under continuous stirring. After 4 h, the white product that had separated was filtered off, washed with water, followed by diethyl ether, and dried. The crude mass was dissolved in CH_2Cl_2; insoluble material, if any, was removed by filtration, and the solvent evaporated. A CH_2Cl_2 solution of this material was subjected to gas chromatography, and the identity of the products confirmed by GC–MS. Table 2 gives an overview of the percentage conversion as a function of varying amounts of $HClO_4$, with all of the other parameters kept constant.

Table 2 Effect of the amount of $HClO_4$ on the oxidative bromination of salicylaldehyde[a]

Complex	[HClO$_4$]/mmol	Conversion[b] (%)
3	2	42.1
	3	46.8
	4	51.5
	5	51.0
6	2	38.6
	3	49.2
	4	50.8
	5	50.0

[a] Reaction conditions: Salicylaldehyde (2 mmol), H_2O_2 (15 mmol), complex (0.02 g, *ca.* 0.05 mmol) and KBr (4 mmol). [b] Average of three different reactions using fresh catalyst each time.

Oxidation of benzene. Complexes **3** and **6** have also been employed to carry out the oxidation of benzene. Benzene (3.9 g, 50 mmol), 30% aqueous H_2O_2 (5.67 g, 50 mmol) and catalyst (0.025 g, *ca.* 0.07 mmol) were taken in 5 ml of acetonitrile and the reaction mixture was heated at 80 °C in an oil bath with stirring. The reaction product was analysed by GC, by withdrawing small aliquots from the reaction mixture after specific intervals of time. To evaluate the effect of the oxidant, the amount of H_2O_2 was varied while keeping the other conditions constant.

Oxidation of phenol. Phenol (4.7 g, 50 mmol) and 30% aqueous H_2O_2 (5.67 g, 50 mmol) were mixed in 5 ml of acetonitrile and the reaction mixture was heated to 80 °C in an oil bath with stirring. After addition of complex **3** or **6** (0.025 g), the stirring was continued. The reaction product was analysed as described above.

Results and discussion

Synthesis, reactivity and solid state characteristics

Scheme 2 provides an overview of the complexes discussed in this paper. Reaction of [VO(acac)$_2$] with an equimolar amount of the ligand H_2sal-nah (**I**) or H_2sal-fah (**II**) in dry refluxing methanol yielded the oxovanadium(IV) complex [VO(sal-nah)H_2O], **1**, or [VO(sal-fah)H_2O], **4**. The ligands coordinate out of their dianionic (ONO(2−)) enolate tautomeric form; *cf.* Scheme 1. The complexes **1** and **4** exhibit effective magnetic moments of 1.47 and 1.54 μ_B, respectively, at 298 K, which is subnormal with respect to the expected value of 1.73 μ_B for a d^1 ($S = \frac{1}{2}$) system. We studied the magnetic susceptibility of **1** as a function of temperature in the 298–78 K range; Fig. S1 (see ESI†). The magnetic moment is slightly dependent on temperature, the range being 1.47–1.40 μ_B. The Curie–Weiss plot [$1/\chi_m$ *vs.* T] is a straight line with a Weiss constant of −11 indicating weak antiferromagnetic interaction. A possible explanation for the antiferromagnetic behaviour is dimerisation (or oligomerisation) of the complex molecules *via* V=O···V interaction.

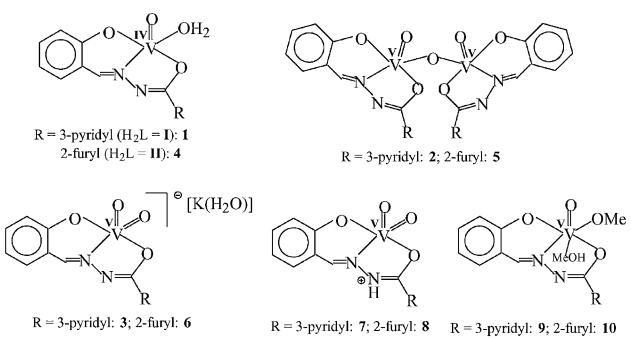

Scheme 2

On aerial oxidation of [VO(sal-nah)H_2O] in methanol, the dioxovanadium(V) complex [{VO(sal-nah)}$_2$μ-O], **2**, was obtained. The amount of solvent and duration of crystallisation plays an important role, in that an excess of solvent and prolonged crystallisation periods cause partial deoxygenation of **2**, leading to the species [VO(OMe)(MeOH)(sal-nah)], **9**. Similarly, [VO(sal-fah)H_2O] can be oxidised to [{VO(sal-fah)}$_2$μ-O], which can further be transformed into [VO(OMe)(MeOH)(sal-fah)], **10**. Eqns (1), (2) and (3) represent the overall synthetic procedures.

$$[V^{IV}O(acac)_2] + H_2\text{sal-nah} \rightarrow \underset{\mathbf{1}}{[V^{IV}O(\text{sal-nah})H_2O]} + 2\,\text{Hacac} \quad (1)$$

$$2[V^{IV}O(\text{sal-nah})H_2O] + \tfrac{1}{2}O_2 \rightarrow \underset{\mathbf{2}}{[\{V^{V}O(\text{sal-nah})\}_2\mu\text{-O}]} + 2H_2O \quad (2)$$

$$[\{V^{V}O(\text{sal-nah})\}_2\mu\text{-O}] + 4\,\text{MeOH} \quad (\mathbf{2})$$
$$\rightarrow 2\,[V^{V}O(OMe)(MeOH)(\text{sal-nah})] + H_2O \quad (\mathbf{9}) \qquad (3)$$

A solution of potassium vanadate (which, at ambient pH, is actually present as a mixture of vanadates), generated *in situ* by dissolving V_2O_5 in aqueous KOH, reacts with the potassium salts of **I** and **II** at pH *ca.* 7.5 to give the potassium salts of the dioxovanadium(V) anions, $[K(H_2O)][VO_2(\text{sal-nah})]$, **3**, and $[K(H_2O)][VO_2(\text{sal-fah})]$, **6**; eqn. (4).

$$K[VO_3] + K_2L \rightarrow [K(H_2O)][V^{V}O_2L]\ (H_2L = \mathbf{I}\text{: }\mathbf{3},\ H_2L = \mathbf{II}\text{: }\mathbf{6}) \qquad (4)$$

Aqueous solutions of **3** and **6** further react with $HClO_4$ to yield the neutral complexes $[VO_2(\text{Hsal-nah})]$, **7**, and $[VO_2(\text{Hsal-fah})]$, **8**, in which one of the nitrogens of the =N–N= group is protonated (see also Plass *et al.*[28]); eqn. (5).

$$[K(H_2O)][V^{V}O_2L] + HClO_4 \rightarrow [V^{V}O_2(HL)] + KClO_4 + H_2O \quad (\mathbf{3/6} \rightarrow \mathbf{7/8}) \qquad (5)$$

Slow crystallisation of **7** and **8** from excess methanol causes the removal of the proton from the NH group and conversion to the methoxo-oxovanadium(V) complexes **9** and **10**; eqn. (6).

$$2[V^{V}O_2HL] + 2\,\text{MeOH} \rightarrow [V^{V}O(OMe)(MeOH)L] + H_2O \quad (\mathbf{7/8} \rightarrow \mathbf{9/10}) \qquad (6)$$

The formation of the complexes **9** (L = sal-nah(2−)) and **10** (L = sal-fah(2−)) from the corresponding neutral mono- or dinuclear dioxovanadium(V) complexes in methanol is of interest in the context of vanadium complexes used as oxo-transfer agents both in catalytic and stoichiometric oxygenation reactions.[33]

All of the complexes are soluble in methanol, ethanol, DMSO and DMF; the anionic complexes **3** and **6** are additionally soluble in water. The structures of the complexes as depicted in Scheme 2 are based on the spectroscopic (IR, UV-Vis, EPR, ^{1}H, ^{13}C and ^{51}V NMR) data, thermogravimetric patterns, magnetic susceptibility measurements, elemental analyses, and X-ray diffraction analyses in the case of **9** and **10**.

IR patterns of the complexes correspond to those observed in other oxo-hydrazonatovanadium complexes;[1] for a detailed description see ESI† (IR spectra).

Thermal studies

The complexes $[VO(\text{sal-nah})H_2O]$ and $[VO(\text{sal-fah})H_2O]$ lose weight between 100 and 160 °C equivalent to one water molecule, indicative of relatively weakly coordinated water. Further increase of the temperature causes weight loss between 250 and 450 °C in two overlapping steps, corresponding to the loss of the organic ligand minus one oxygen. The end product of the thermal decomposition is V_2O_5. The dioxovanadium(V) complexes $[K(H_2O)][VO_2(\text{sal-nah})]$ and $[K(H_2O)][VO_2(\text{sal-fah})]$ lose weight in the temperature range 150–220 °C due to the loss of one water, which we attribute to water coordinated to K^+. The water-free species $K[VO_2(\text{sal-nah})]$ further decomposes in two overlapping steps in the temperature range 280–440 °C, while decomposition of $K[VO_2(\text{sal-fah})]$ occurs in multiple overlapping steps between 250 and 650 °C to form potassium metavanadate $K[VO_3]$. The total weight loss in both complexes corresponds to the loss of ligand minus one oxygen. The decomposition patterns of $[\{VO(\text{sal-nah})\}_2\mu\text{-O}]$ and $[\{VO(\text{sal-fah})\}_2\mu\text{-O}]$ could not be followed in detail due to multiple overlapping decomposition steps in the temperature range 200–500 °C. The end product is close to V_2O_5 in either case. Complex $[VO_2(\text{Hsal-nah})]$ is stable up to 275 °C, and thereafter decomposes in three steps yielding V_2O_5 at 480 °C (obs: 27.7, cal: 28.2%). Similarly, $[VO_2(\text{Hsal-fah})]$ decomposes in several steps between 190 and 500 °C to give V_2O_5 (obs: 28.3, cal: 29.2%).

EPR studies

Complexes **1** and **4** exhibit an axial low temperature spectrum typical of tetragonal-pyramidal oxovanadium(IV) complexes, *i.e.* two sets of eight lines (coupling of the single electron with the ^{51}V spin 7/2 nucleus) corresponding to the parallel (z) and perpendicular (xy) components of the g and hyperfine coupling (A) tensors. No rhombic distortion was observed. The g values of **1** and **4** ($g_{xy} = 1.979$, $g_z = 1.948$) and the hyperfine coupling constants ($A_{xy} = 58.0$, $A_z = 166.0 \times 10^{-4}$ cm^{-1}) are in accord with the O_3N donor sets. The parallel hyperfine coupling constant A_z is close to the value calculated from the partial contributions of the equatorial ligand set (H_2O, enolate(1−), phenolate(1−), imine-N), $A_z(\text{calcd.}) = 162.2 \times 10^{-4}$ cm^{-1}.[34]

Structure description

The molecular structures of the oxo-methoxo complexes **9** and **10** along with the numbering schemes are shown in Fig. 1. Table 3 contains selected bond lengths and angles. The coordination geometry around vanadium can be described as tetragonal-bipyramidal, with the doubly bonded oxygen and methanol in the axial positions. The O=V–O(methanol) axis is almost linear; the angle at vanadium is 175.39(5)° in **9** and 173.4(2)° in **10**. Because of the *trans* influence of the oxo group, the distance to methanol, d(V–O5) (2.2514(10) in **9**, 2.3081(5) Å in **10**) is considerably elongated, making the methanol a weakly coordinated ligand. Such elongation has previously been observed in other complexes with similar structures.[23–29] The phenolate and enolate oxygens, the methoxide and the imine nitrogen define the tetragonal plane, from which vanadium deviates by 0.2790 Å in **9** and 0.2884 Å in **10**. The O–C, N–C and N–N distances are consistent with the enolate form of the corresponding functionality. Other bond lengths, and the bond angles, are similar to those observed in comparable complexes.[23–29,35–37] Except for the non-coordinated N1, the atoms maintain sp^2 planarity. In **10**, N1 is involved in intermolecular hydrogen bonding to the proton of the coordinated methanol *trans* to the oxo group, $d(\text{N1}\cdots\text{O5}) = 2.795$ Å (**10**). In addition, there are close intermolecular O···H–C contacts between the enolate-O (O2) and C10 of the sal moiety in **10**, $d(\text{O2}\cdots\text{C10}) = 2.459$ Å. The methanol-OH in **9** forms a hydrogen bond to the pyridine-N (N3) of an adjacent molecule, $d(\text{O5}\cdots\text{N3}) = 2.792$ Å.

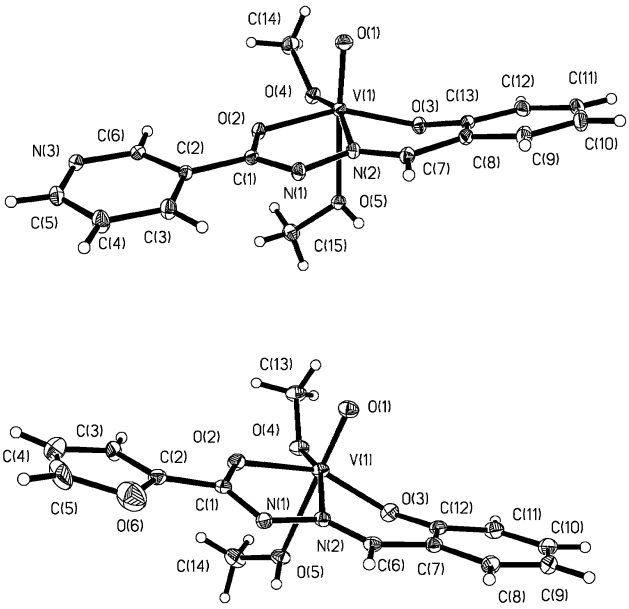

Fig. 1 ORTEP plot (at the 30% probability level) of [VO(OMe)(MeOH)(sal-nah)] (**9**) (top) and [VO(OMe)(MeOH)(sal-fah)] (**10**) (bottom).

Table 3 Selected bond lengths [Å] and bond angles [°] for **9** and **10**

	9	10		9	10
V1–O1	1.5943(10)	1.593(2)	O1–V1–O5	175.39(5)	175.66(9)
V1–O2	1.9559(9)	1.976(2)	O4–V1–O3	105.53(4)	102.92(9)
V1–O3	1.8598(9)	1.851(2)	O4–V1–O2	91.84(4)	93.55(9)
V1–O4	1.7764(9)	1.769(2)	O3–V1–O2	151.36(4)	152.61(9)
V1–O5	2.2514(10)	2.295(2)	O4–V1–N2	162.09(4)	161.73(10)
V1–N2	2.1282(11)	2.122(3)	O3–V1–N2	83.66(4)	83.66(9)
N1–C1	1.3081(15)	1.304(4)	O2–V1–N2	74.14(4)	74.56(9)
N1–N2	1.3929(14)	1.394(3)	C1–N1–N2	107.52(9)	108.7(2)
N2–C7/6	1.2939(15)	1.281(4)	C7/6–N2–N1	116.50(10)	116.9(2)
O2–C1	1.3004(14)	1.302(3)	N2–C7/6–C8/7	123.111(11)	123.4(3)
			N1–C1–O2	123.92(10)	123.6(3)

Solution studies

^{1}H NMR studies. The relevant data are presented in Table S1 (ESI†). Both of the free ligands give rise to a signal at δ = 11.20 due to the –NH proton, indicating their existence in the ketonic form. The absence of this signal in the complexes is in accord with enolisation and subsequent replacement of H by the metal ion. Similarly, the absence of the signal for the phenolic OH (*ca.* 12.2 ppm in the ligands) indicates coordination of phenolate oxygen. A significant downfield shift of the azomethine (–CH=N–) proton signal in the complexes with respect to the corresponding free ligands confirms the coordination of the azomethine nitrogen. The ^{1}H NMR data are thus consistent with the ONO dibasic tridentate binding mode of the ligands. The aromatic protons of ligands and complexes appear in the expected region. In the case of the dinuclear complexes **2** and **5**, speciation appears to occur in CD_3OD, as two sets of signals were observed for several of the protons. One set of signals corresponds to **2** and **5**, while the other, minor set (not shown in Table S1), belongs to a second species (see also ^{13}C and ^{51}V NMR). Similarly, solutions of [VO_2(Hsal-fah)] (**8**) exhibit two signals for the azomethine proton at δ = 8.92 and 8.84 in the ratio of 6.5 : 1 (freshly prepared) or 1 : 1.8 (recrystallised from methanol), indicating slow conversion of **8** to **10**.

^{13}C NMR studies. We have also recorded ^{13}C NMR of ligand **II** and its complexes to provide diagnostic tools for the elucidation of the structures. Assignments of the peaks are similar to those reported earlier, and are based on the chemical shift and intensity patterns. Table S2 (ESI†) presents the data along with the coordination induced shifts $\Delta\delta$ = δ(complex) − δ(ligand) of the signals for carbon atoms in the vicinity of the coordinating functions. A large $\Delta\delta$ observed for carbon atoms in the vicinity of the phenolate (C3), enolate (C8) and azomethine (C1) groups suggests their involvement in coordination. Two new signals in sample **8** recrystallised from methanol appear at δ = 48.5 and 74.3 ppm. These signals correspond to methanol and methoxy carbon atoms, respectively, testifying partial conversion of [VO_2(Hsal-fah)] (**8**) to [VO(OMe)(MeOH)(sal-fah)] (**10**).

^{51}V NMR studies. δ(^{51}V) values of the complexes are contained in the Experimental section. The resonances are somewhat broadened due to nuclear quadruple relaxation (I(^{51}V) = 7/2)); line widths at half height are typically around 200 Hz. The dioxovanadium(V) complexes **3** and **6** show one strong resonance at δ = −532.4 (**3**) and at δ = −533.9 (**6**), which is close to the one reported for [K(H_2O)][VO_2(sal-inh)] (−532.0 ppm)[38] and the expected shift for dioxovanadium(V) complexes containing a mixed O/N donor set.[39,40] The appearance of two signals at δ = −542.4 and −584.6 for [{VO(sal-nah)}$_2$μ-O] (**2**) in a ratio of 4 : 1 indicates the presence of two species. The major signal at −542.4 ppm is assigned to **2**. The nature of the minor, high-field signal remains elusive. A possible candidate is [VO(OH)(sal-nah)] formed by reaction of **2** with the water present in DMSO. In CD_3OD, the two signals appear at δ = −541.7 and −550.1, corresponding to the dinuclear complex **2** and the oxo-methoxo complex [VO(OMe)(MeOD)(sal-nah)], **3**. The complex [{VO(sal-fah)}$_2$μ-O] (**5**) displays three signals at δ = −538.7 (**5**), −550.5 (**10**) and −583.5.

Electronic absorption spectra. The data for the ligands and complexes are listed in Table S3 (ESI†). The UV spectrum of H_2sal-nah (**I**) exhibits four absorption bands at 214, 288.5, 297.5 and 328 nm, while H_2sal-fah (**II**) shows bands at 211.5, 288.5, 299 and 328 nm. The most probable assignments of the first and last bands are $\phi \rightarrow \phi^*$ and $n \rightarrow \pi^*$ transitions, respectively, while the two remaining bands are $\pi \rightarrow \pi^*$ transitions. A weak shoulder associated with the first band is due to hydrogen bonding. In all of the complexes, this shoulder disappears, and the split $\pi \rightarrow \pi^*$ band merges into one, while the other bands invariably are present. The $\phi \rightarrow \phi^*$ band has no definite trend, while the other two bands are generally shifted towards lower wavelengths in comparison to the uncoordinated ligands. In addition, all of the complexes display a medium intensity band at 396–409 nm, which is assigned to a ligand-to-metal charge transfer (LMCT) from the phenolic oxygen to an empty d-orbital of the vanadium ion. The oxovanadium(IV) complexes **1** and **4** exhibit one broad but well-developed band at *ca.* 405 nm. This is similar to the absorption reported for [VO(hydrox-atp)H_2O] (H_2hydrox-atp = Schiff base derived from 2-hydroxy-1-naphthaldehyde and 2-aminothiophenol) and is considered to be a $d \rightarrow d$ transition.[41]

Reaction of 3 and 6 with $HClO_4$. Drop-wise addition of $HClO_4$ (dissolved in the minimum amount of methanol) to [K(H_2O)][VO_2(sal-fah)] (**6**) in methanol (*cf.* Fig. 2) causes darkening of the solution with an increase in intensity of the UV bands, and a decrease in the intensity and shift of the 396 nm band to 406.5 nm. The UV bands at 282.5, 301 and 324 nm

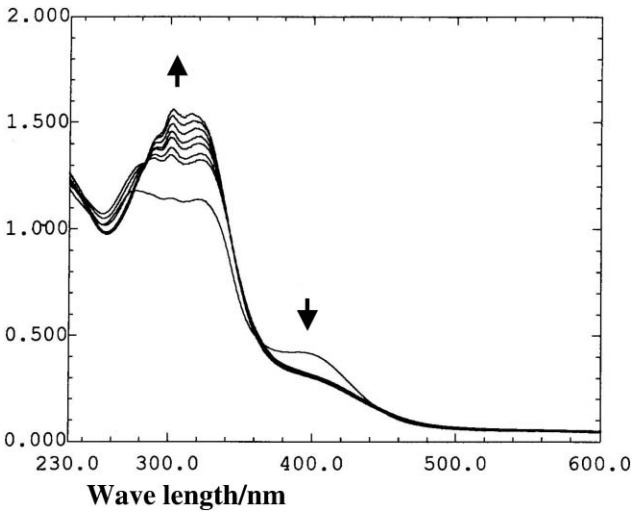

Fig. 2 Titration of [K(H_2O)][VO_2(sal-fah)] **6** with a saturated solution of $HClO_4$ in MeOH; the spectra were recorded after addition of 2-drop portions of MeOH–$HClO_4$ to 10 ml of *ca.* 10^{-4} M solution of **6** in MeOH.

finally merge into two bands at 300 and 318 plus a shoulder at 290 nm. Corresponding results have been obtained with a saturated solution of HCl gas in methanol. A reduction in the intensity of the 395.5 nm band and an increase of the 320 and 231 nm bands along with their shift have also been observed for $[K(H_2O)][VO_2(sal\text{-}nah)]$ (**3**): The 395.5 nm band shifts to 405 nm and broadens, while the 320 and 231 nm bands shift to 326 and 253 nm.

We interpret these result in terms of the formation of oxohydroxo complexes of composition $[VO(OH)(HL)]^+$ *via* $[VO_2(HL)]$ (eqn. (7)),

$$[VO_2(L)]^- \overset{H^+}{\rightarrow} [VO_2(HL)] \overset{H^+}{\rightarrow} [VO(OH)(HL)]^+ \qquad (7)$$

with one of the =N–N= nitrogens being the site of protonation; see **7** and **8** in Scheme 2. This assumption is based on the similarity between the electronic spectra of freshly prepared methanolic solutions of **7** and **8**, and the spectra obtained for **3** and **6** after addition of the first portion of $HClO_4$ or HCl. Protonation of the hydrazone nitrogen has been reported, *e.g.* for the structurally characterised complex [VO(Hsal-bhz)] (H_2sal-bhz derives from salicylaldehyde and benzoylhydrazide), which forms on treatment of the corresponding anionic dioxo complex with HCl.[28]

Oxo-hydroxovanadium complexes have previously been generated on acidification of $K[VO_2(sal\text{-}inh)H_2O]$ (H_2sal-inh = hydrazone derived from salicylaldehyde and isonicotinic acid hydrazide) and $[K(H_2O)_2][VO_2(Clsal\text{-}sbdt)]$ (H_2Clsal-sbdt = ligand derived from 5-chlorosalicylaldehyde and *S*-benzyldithiocarbazate).[20] An oxo-hydroxo complex, $[VO(OH)(LH)]^+$ (where LH = *N*-{(*o*-hydroxyphenyl)methyl}-*N*′-bis(2-hydroxyethyl)ethylenediamine) in solution has also been reported to form from a dinuclear dioxovanadium(V) precursor in a similar manner.[42] $[V^VO(OH)(8\text{-oxyquinolinate})_2]$[43] and $[V^{IV}O(OH)Tp(H_2O)]$ [Tp = tris(3,5-diisopropyl-1-pyrazolyl)borate(1−)][44] have been characterised in the solid state. On addition of a methanolic solution of KOH to $[VO(OH)(Hsal\text{-}nah)]^+$ or $[VO(OH)(Hsal\text{-}fah)]^+$, the solution acquired the original spectra of **3** or **6**; the reaction is thus reversible. This reversibility is an important observation in the context of the active site structure and the catalytic activity of vanadate-dependent haloperoxidases, for which an apical hydroxo ligand at the vanadium centre has been derived from X-ray diffraction evidence,[45] and also suggested on the basis of kinetic investigations.[7,8]

Reaction of 3 and 6 with H_2O_2. The formation of peroxo complexes in methanol by treatment of $[VO_2L]^-$ with H_2O_2 could be established by electronic absorption and ^{51}V NMR spectroscopies: Treatment of 10 ml of a *ca.* 0.5×10^{-4} solution of $[K(H_2O)][VO_2(sal\text{-}nah)]$ (**3**) with 2-drop portions of 30% H_2O_2 dissolved in methanol resulted in the UV-Vis spectra recorded in Fig. 3. The band for $[VO_2(sal\text{-}nah)]^-$ at 397.5 nm shifts to 404.5 nm along with a decrease in intensity. The two bands appearing at 318.5 and 282.5 nm slowly merge into one and appear as a shoulder of a strong absorption at *ca.* 230 nm (not shown). The amount of peroxo complex formed depends upon the amount of H_2O_2 added. Exactly the same pattern is observed for **6**, where the 394.5 nm band shifts to 400.5 nm, and the 319.0, 299.5 and 286.5 nm bands merge into a shoulder. The ^{51}V NMR spectrum of $[K(H_2O)][VO_2(sal\text{-}fah)]$ (**6**) in DMSO/H_2O plus a small amount of $HClO_4$ and H_2O_2, *i.e.* under conditions where peroxo complexes should form and be fairly stable, resulted in the appearance of an additional peak at −575 along with the original signal at −538 ppm. The signal at −575 ppm should reflect the presence of an oxomonoperoxo species. The peroxo ligand usually gives rise to an upfield shift of 40–60 ppm with respect to the parent dioxovanadium(V) complex.[46]

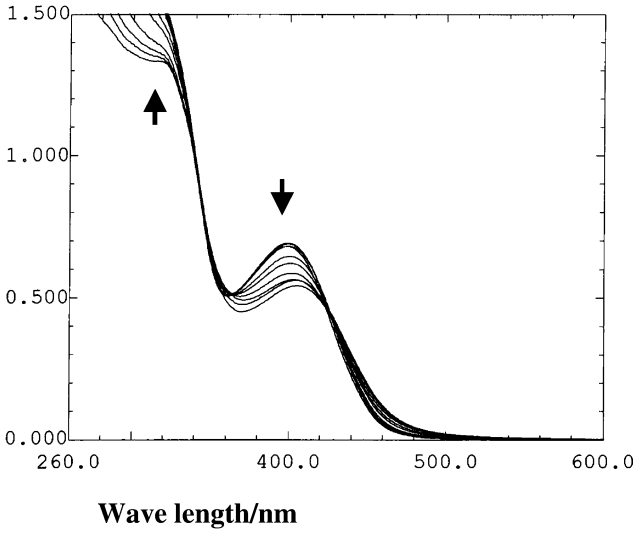

Fig. 3 Titration of $[K(H_2O)][VO_2(sal\text{-}nah)]$ **3** with 30% H_2O_2; the spectra were recorded after the successive addition of 2-drop portions of H_2O_2 to 10 ml of a *ca.* 0.5×10^{-4} M solution of **3** in MeOH.

Catalytic activity studies

Oxidative bromination of salicylaldehyde. As pointed out in the Introduction, vanadate-dependent bromoperoxidases catalyse the bromination of organic substrates in the presence of H_2O_2 and bromide, and the ability of vanadium compounds to mimic this reaction has been demonstrated. Examples are the bromination of trimethoxybenzene by the VO_2^+ ion,[47] and the bromination of phenol red by $[VO(O_2)H_2O]^+$ and related species.[48] In the following section we show, for complexes **3** and **6**, that they catalyse oxidative bromination of salicylaldehyde, benzene and phenol, using aqueous H_2O_2/KBr in the presence of $HClO_4$; *cf.* eqn. (8).

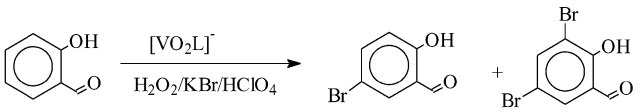

(8)

Oxidative bromination with H_2O_2/KBr catalysed by V_2O_5 and oxovanadium(V) complexes[19b] has shown that, during this process, vanadium reacts with one or two equivalents of H_2O_2, forming monoperoxo $\{VO(O_2)^+\}$or bis(peroxo) $\{VO(O_2)_2^-\}$ species, which ultimately oxidise bromide, possibly *via* a hydroperoxo intermediate. The oxidised bromine species (Br_2, Br_3^- and/or HOBr) then brominates the substrate.[4,49]

In order to achieve optimum conditions, both catalysts (**3** and **6**) were studied in detail by varying parameters such as the volume of $HClO_4$ (see Experimental section), the amount of catalyst and of H_2O_2 at ambient temperature. Maximum conversion of salicylaldehyde (*ca.* 51%) was achieved with 4 mmol of $HClO_4$, 2 mmol of substrate, 15 mmol of H_2O_2, 20 mg (*ca.* 0.05 mmol) of catalyst and 0.476 g (4 mmol) of KBr. GC and GC-MS analysis of the crude products obtained under optimised conditions gave 85.8% 5-bromosalicylaldehyde, 9.0% 3,5-dibromosalicylaldehyde and 5.2% of other, unidentified, products. The turn over rate per hour (TOF h^{-1} = moles of substance converted per mole of catalyst per hour) is about 5, which compares to what has been reported for the complex $[K(H_2O)_3][VO_2(pydx\text{-}inh)]$ (pydx-inh is the hydrozone from pyridoxal and isonicotinic acid hydrazide) (46% conversion).[20c] Examples for turn over rates previously reported for model systems are 0.15 (bromination of trimethoxybenzene by VO^{2+} at pH 3)[47] and 32 h^{-1} (with polymeric oxovanadium(IV) complexes of Schiff bases derived from 5,5′-methylenebis(salicylaldehyde) and diamines).[50] In the absence of the catalyst, the reaction mixture did not produce any brominated product demonstrating

the catalytic role of the dioxovanadium(v) complexes. Similarly, acid (here $HClO_4$) was found to be essential to carry out catalytic bromination. The complexes slowly decompose during the reaction when larger amounts of $HClO_4$ (5 mmol or more) were employed. This decomposition could, however, be minimised if $HClO_4$ was added successively in about 4–5 equal portions. Non-oxidising acids, *e.g.* H_2SO_4, give rise to similar results in the conversion of salicylaldehyde.

The formation of oxohydroxo species such as $[VO(OH)HL]^+$ is likely to occur upon acidification of $[VO_2L]^-$ (see above), and the corresponding oxoperoxo species $[VO(O_2)L]^-$/$[VO(HO_2)L]$ should form upon treatment with H_2O_2 in acidic methanol, thus providing the active species necessary for the catalytic reaction. Activation of peroxide by coordination to vanadium thus may be succeeded by formation of an (intermediate) hydroperoxo complex, which allows nucleophilic attack of the bromide,[4] followed by release of hypobromous acid, which then brominates organic substrates. A hypobromite intermediate may also be involved, as evidenced by electron spray ionization mass spectra on model systems.[51] A catalytic cycle is proposed in Scheme 3.

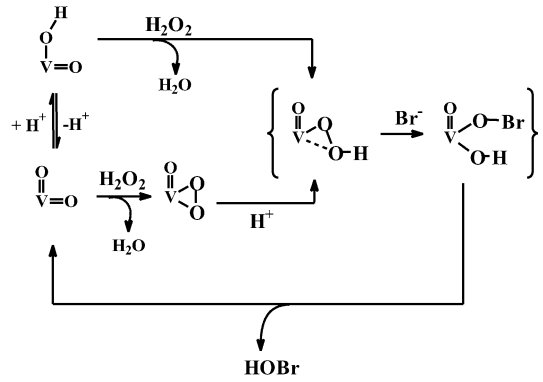

Scheme 3

Oxidation of benzene and phenol. Oxidation of benzene to phenol was also catalysed by **3** and **6**. The effect of the amount of H_2O_2 on the oxidation of benzene to phenol is shown in Table 4. At a molar ratio benzene : H_2O_2 = 1 : 1, 24.2% benzene is converted to phenol within 15 h in the presence of **3**. Lowering the ratio to 1 : 0.5 decreases the conversion considerably (8.6%), while increasing the ratio to 1 : 2 increases this conversion to 28.0%. However, the percentage efficiency of H_2O_2 for a 1 : 2 is lower than for a 1 : 1 molar ratio. Similarly, complex **6** gave 28.3% benzene conversion at a 1 : 1 (benzene to oxidant) molar ratio and 34.5% at a 1 : 2 molar ratio. No further conversion was noticed after 15 h of contact time. It is interesting to note that, under the reaction conditions applied here, no oxidation beyond the formation of phenol was observed.

Complexes **3** and **6** are also able to catalyse the oxidation of phenol to give two major products, *viz.* catechol and *p*-hydroquinone; eqn. (9),

Table 4 Effect of H_2O_2 on percentage conversion of benzene[a]

Complex	Amount of oxidant/g (mmol)	% Conversion (%) 3 h	6 h	15 h
3	2.83 (25)	3.0	5.9	8.6
	5.67 (50)	10.4	17.9	24.2
	11.34 (100)	12.7	22.3	28.0
6	2.83 (25)	7.9	9.5	10.3
	5.67 (50)	12.5	15.3	28.3
	11.34 (100)	17.3	21.0	34.5

[a] Reaction conditions: 50 mmol benzene, 25 mg (*ca.* 0.07 mmol) catalyst, 5 ml CH_3CN; 80 °C.

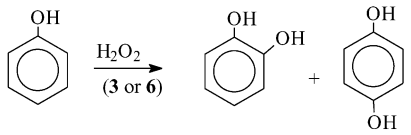

(9)

i.e. the expected products according to the directing effect of the phenolic OH group. In order to achieve suitable reaction conditions for the maximum oxidation of phenol, we studied the following parameters in detail: effect of amount of catalyst, effect of H_2O_2 concentration (moles of H_2O_2 per mole of phenol) and effect of phenol concentration (moles of phenol per mole of H_2O_2). Under optimised reaction conditions (50 mmol substrate, 50 mmol 30% aqueous H_2O_2, 0.07 mmol catalyst in 5 ml of CH_3CN at 80 °C)[52] and 15 h of contact time, 20.1% conversion of phenol to 11.2% catechol and 8.9% hydroquinone is observed with **3** as the catalyst, while the conversion rate is 32.6% (producing 18.0% catechol and 14.6% hydroquinone) in the case of **6**. The corresponding turn over rates per hour were 3 and 5, respectively, for 5 h of contact time, a time interval where 90% of the overall conversion was achieved. Only minor changes in either conversion rate or product composition were observed for reaction times beyond 15 h. In the absence of catalyst, both of these oxidation reactions did not proceed.

Conclusion

Vanadium complexes of general composition $[V^{IV}O(H_2O)L]$, $[\{V^{V}OL\}_2\mu\text{-}O]$, $[K(H_2O)][V^{V}O_2L]$, $[V^{V}O_2HL]$ and $[V^{V}O(OMe)(MeOH)L]$ have been synthesised and characterised, and the molecular structures of $[VO(OMe)(MeOH)L]$ revealed by single crystal X-ray diffraction analyses. L is a dianionic ONO hydrazone ligand derived from salicylaldehyde (sal) and the hydrazides of nicotinic acid (nah) and 2-furanecarbonic acid (fah), *i.e.* of common constituents of physiologically relevant compounds and metabolites thereof. The general overall co-ordination environment is represented by an O_4N donor set: the ONO ligand, the doubly bonded oxo group and an aqua, methoxo or bridging oxo ligand The complexes thus model structural features of the vanadate-dependent haloperoxidases from marine algae (such as *Ascophyllum nodosum* and *Corallina officinalis*) and the fungus *Curvularia inaequalis*. The model character extends to the simulation of the functions of the enzymes in that the complexes $[K(H_2O)][VO_2L]$ catalyse the oxidative bromination of salicylaldehyde by H_2O_2 to afford 5-bromo and 3,5-dibromosalicylaldehyde, and the oxidation of (oxo transfer to) phenol to yield catechol and *p*-hydroquinone. Turn over rate in strongly acidic solution is 5 mol of brominated compound (mol of vanadium complex)$^{-1}$ h^{-1}; the complex is thus substantially less active than the enzyme which, at pH 6.5, exhibits *ca.*10^5 mol of brominated product (mol of enzyme)$^{-1}$ h^{-1}.[47] The formation of intermediates proposed for the catalytic cycle, *i.e.* oxo-hydroxo complexes $[VO(OH)HL]^+$ and oxo-peroxo complexes $[VO(O_2)L]^-$, has been made plausible on the basis of characteristics in the UV-Vis spectra of the anionic dioxovanadium precursor compounds $[VO_2L]^-$ treated with acid and hydrogen peroxide, respectively.

Acknowledgements

We acknowledge performance of the micro-analyses by the Regional Sophisticated Instrumental Centre, CDRI, Lucknow and GC analysis by the Institute Instrumentation Centre of IIT Roorkee. Financial assistance from the Department of Science and Technology, Government of India (Grant No. SP/S1/F-07/2001), New Delhi, and the Deutsche Forschungsgemeinschaft (grant RE 431/20-1) are gratefully acknowledged.

References

1 M. R. Maurya, *Coord. Chem. Rev.*, 2003, **237**, 163.

2 (*a*) D. Rehder, *Coord. Chem. Rev.*, 1999, **182**, 297; (*b*) D. Rehder, in *Metal ions in biological systems*, eds. H. Sigel and A. Sigel, Marcel Dekker, New York, 1995, ch. 1; (*c*) D. Rehder, *Inorg. Chem. Commun.*, 2003, **6**, 604.
3 D. C. Crans, J. J. Smee, E. Gaidamauskas and L. Yang, *Chem. Rev.*, 2004, **104**, 849.
4 A. Butler, *Coord. Chem Rev.*, 1999, **187**, 17.
5 M. Weyand, H.-J. Hecht, M. Kieb, M.-F. Liaud, H. Vilter and D. Schomburg, *J. Mol. Biol.*, 1999, **293**, 595.
6 M. I. Isupov, A. R. Dalby, A. A. Brindley, Y. Izumi, T. Tanabe, G. N. Murshdov and J. A. Littlechild, *J. Mol. Biol.*, 2000, **299**, 1035.
7 G. J. Colpas, B. J. Hamstra, J. W. Kampf and V. L. Pecoraro, *J. Am. Chem. Soc.*, 1996, **118**, 3469.
8 B. J. Hamstra, G. J. Colpas and V. L. Pecoraro, *Inorg. Chem.*, 1998, **37**, 949.
9 J. A. Littlechild and E. Gorcia-Rodriguez, *Coord. Chem. Rev.*, 2003, **237**, 65.
10 S. Macedo-Ribeiro, W. Hemrika, R. Renirie, R. Wever and A. Messerschmidt, *J. Biol. Inorg. Chem.*, 1999, **4**, 209.
11 A. Messerschmidt and R. Wever, *Proc. Natl. Acad. Sci. USA*, 1996, **93**, 392.
12 C. Hiort, J. Goodisman and J. C. Dabrowiak, *Biochemistry*, 1996, **35**, 12354.
13 Y. Zhang and R. H. Holm, *Inorg. Chem.*, 1990, **29**, 911.
14 I. W. C. E. Arends, M. P. Birelli and R. A. Sheldon, *Stud. Surf. Catal.*, 1997, **110**, 1031.
15 H. B. ten Brink, H. E. Schoemaker and R. Wever, *Eur. J. Biochem.*, 2001, **268**, 132.
16 C. Bolm and F. Bienewald, *Angew. Chem., Int. Ed. Engl.*, 1996, **34**, 2640.
17 G. Santoni, G. M. Licini and D. Rehder, *Chem. Eur. J.*, 2003, **9**, 4700.
18 T. S. Smith, II and V. L. Pecoraro, *Inorg. Chem.*, 2002, **41**, 6754.
19 (*a*) V. Conte, F. D. Furia and G. Licini, *Appl. Catal. A*, 1997, **157**, 335; (*b*) A. G. J. Ligtenbarg, R. Hage and B. L. Feringa, *Coord. Chem. Rev.*, 2003, **237**, 89.
20 (*a*) M. R. Maurya, S. Khurana, W. Zhang and D. Rehder, *J. Chem. Soc., Dalton Trans.*, 2002, 3015; (*b*) M. R. Maurya, S. Khurana, W. Zhang and D. Rehder, *Eur. J. Inorg. Chem.*, 2002, 1749; (*c*) M. R. Maurya, S. Agarwal, C. Bader and D. Rehder, *Eur. J. Inorg. Chem.*, 2005, 147.
21 W. Plass, *Coord. Chem. Rev.*, 2003, **237**, 205.
22 K. Nakajima, M. Kojima, K. Toriumi, K. Saito and J. Fujita, *Bull. Chem. Soc. Jpn.*, 1989, **62**, 760.
23 M. J. Clague, N. L. Keder and A. Butler, *Inorg. Chem.*, 1993, **32**, 4754.
24 S. Dutta, S. Mondal and A. Chakravorty, *Polyhedron*, 1995, **14**, 1163.
25 G. Asgedom, A. Sreedhara, J. Kivikoski and C. P. Rao, *Polyhedron*, 1996, **16**, 643.
26 N. R. Sangeetha, V. Kavita, S. Wocadlo, A. K. Powell and S. Pal, *J. Coord. Chem.*, 2000, **51**, 55.
27 M. Moon, M. Pyo, Y. C. Myoung, C. I. Ahn and M. S. Lah, *Inorg. Chem.*, 2001, **40**, 554.
28 W. Plass, A. Pohlmann and H.-P. Yozgatli, *J. Inorg. Biochem.*, 2000, **80**, 181.
29 (*a*) D. Wang, M. Ebel, C. Schulzke, C. Grüning, S. K. S. Hazari and D. Rehder, *Eur. J. Inorg. Chem.*, 2001, 935; (*b*) R. Fulwood, H. Schmidt and D. Rehder, *Chem. Commun.*, 1995, 1443.
30 A. Syamal and M. R. Maurya, *Indian J. Chem., Sect. A*, 1985, **24**, 836.
31 R. A. Row and M. M. Jones, *Inorg. Synth.*, 1957, **5**, 113.
32 R. L. Dutta and A. Syamal, *Elements of Magnetochemistry*, Affiliated East–West Press, New Delhi, 2nd. edn., 1993, p. 8.
33 (*a*) Y. Zhang and R. H. Holm, *Inorg. Chem.*, 1990, **29**, 911; (*b*) T. Hirao, *Chem. Rev.*, 1997, **97**, 2707.
34 (*a*) T. S. Smith, II, R. LoBrutto and V. L. Pecoraro, *Coord. Chem. Rev.*, 2002, **228**, 1; (*b*) A. J. Tasiopoulos, A. N. Troganis, A. Evangelou, C. P. Raptopoulos, A. Terzis, Y. Deligiannakis and T. A. Kabanos, *Chem. Eur. J.*, 1999, **5**, 910.
35 S. Mondal, S. P. Rath, S. Dutta and A. Chakravorty, *J. Chem Soc., Dalton Trans.*, 1996, 99.
36 S. Mondal, S. P. Rath, S. Dutta, K. K. Rajak and A. Chakravorty, *Inorg. Chem.*, 1998, **37**, 1713.
37 S.-X. Liu and S. Gao, *Inorg. Chim. Acta*, 1998, **282**, 149.
38 M. R. Maurya, S. Khurana, C. Schulzke and D. Rehder, *Eur. J. Inorg. Chem.*, 2001, 779.
39 D. Rehder, C. Weidemann, A. Duch and W. Priebsch, *Inorg. Chem.*, 1988, **27**, 584.
40 (*a*) O. W. Howarth, *Prog. Magn. Reson. Spectrosc.*, 1990, **22**, 453; (*b*) D. Rehder, in *Transition Metal Nuclear Magnetic Resonance*, ed. P. S. Pregosin, Elsevier, Amsterdam, 1991, pp. 1–58.
41 C. C. Lee, A. Syamal and L. J. Theriot, *Inorg. Chem.*, 1971, **10**, 1669.
42 G. J. Colpas, B. J. Hamstra, J. W. Kampf and V. L. Pecoraro, *Inorg. Chem.*, 1994, **33**, 4669.
43 A. Giacomelli, C. Floriani, A. O. De Souza Duarte, A. Chiesi-Villa and C. Guastino, *Inorg. Chem.*, 1982, **21**, 3310.
44 M. Kosugi, S. Hikichi, M. Akita and Y. Moro-oka, *Inorg. Chem.*, 1999, **38**, 2567.
45 (*a*) A. Messerschmidt, L. Prade and R. Wever, *Biol. Chem.*, 1997, **378**, 309; (*b*) S. Macedo-Ribeiro, W. Hemrika, R. Renirie, R. Wever and A. Messerschmidt, *J. Biol. Inorg. Chem.*, 1999, **4**, 209.
46 (*a*) M. Časný and D. Rehder, *Dalton Trans.*, 2004, 839–846; (*b*) M. Sivák, M. Mad'orová, J. Taatiersky and J. Marek, *Eur. J. Inorg. Chem.*, 2003, 2075.
47 R. I. de la Rosa, M. J. Clague and A. Butler, *J. Am. Chem. Soc.*, 1992, **114**, 760.
48 R. M. Tóltaro, P. A. M. Williams, M. C. Apella, M. A. Blesa and E. J. Baran, *J. Chem. Soc., Dalton Trans.*, 2000, 4403.
49 (*a*) A. Butler, in *Bioinorganic Catalysis*, eds. J. Reedijk and E. Bouwman, Marcel Dekker, New York, 1999, 2nd ed., ch. 5; (*b*) V. L. Pecoraro, C. Slebodnick and B. Hamstra, in Vanadium Compounds: Chemistry, Biochemistry and Therapeutic Applications, *ACS Symp. Ser.*, eds. D. C. Crans and A. S. Tracy, 1998, ch. 12.
50 M. R. Maurya, A. Kumar, P. Manikandan and S. Chand, *Appl. Catal. A: General*, 2004, **277**, 45.
51 M. Carrano Bortolini, V. Conte and S. Moro, *Eur. J. Inorg. Chem.*, 2003, 42–46.
52 (*a*) M. R. Maurya, I. Jain and S. J. J. Titinchi, *Appl. Catal. A: General*, 2003, **249**, 139; (*b*) M. R. Maurya, H. Saklani, A. Kumar and S. Chand, *Catal. Lett.*, 2004, **93**, 121.